Bounds on Turbulent Transport

Charles R. Doering
Department of Mathematics
University of Michigan
Ann Arbor, MI 48109-1109

with thanks to collaborators

P. Constantin
M. Dontcheva
C. Foias
J. M. Hyman
M. A. Orwoll
J. Otero
E. A. Spiegel
X. Wang
D. P. Wick
R. A. Worthing

Geophysical Fluid Dynamics Fellowships
at the
Woods Hole Oceanographic Institution

2002 Program of Study in Geophysical Fluid Dynamics

Bounds on Turbulent Transport

June 17 to August 23, 2002

Since 1959 the Geophysical Fluid Dynamics (GFD) Program has brought together graduate students and researchers from a variety of fields who share a common interest in the nonlinear dynamics of rotating, stratified fluids. These fields include classical fluid dynamics, physical oceanography, meteorology, astrophysics, planetary atmospheres, geological fluid dynamics, hydromagnetics, physics and applied mathematics. For the graduate student fellows, the centerpiece of the program is a research project that each fellow pursues under the supervision of the staff. At the end of the program, each fellow presents a lecture and a written report for a proceedings volume.

The central topic of the 2002 program will be "Bounds on Turbulent Transport". The introductory lectures by F. H. Busse (University of Bayreuth) will discuss studies of rigorous upper bounds to transports of heat by convection and to momentum by shear flow. The solutions of the associated variational problems share many properties such as temperature profiles or shear flow profiles with actually realized turbulent velocity fields. Topics of rotating convection and turbulence in stratified fluid will be covered in additional lectures during a mini-symposium. The theoretical descriptions of the nonlinear dynamics of these systems share common features with the variational problems such as sequences of successive bifurcations and modification of the mean field. Numerous additional staff lectures will be given in these and other topics during the program. More details of the topics are found at the announcement for 2002 on the web site.

Up to ten competitive fellowships are available for graduate students. Successful applicants will receive stipends of $4.275 and an allowance for travel expenses within the United States. Fellows are expected to be in residence for the full ten weeks of the program. The application deadline is February 15, 2002. Awards will be announced by April 1, 2002. We particularly encourage applications from women and members of underrepresented groups. Further information and application forms may be obtained through the Education section of the Woods Hole Oceanographic Institution World Wide Web homepage at http://www.whoi.edu/education/gfd.html, or by writing directly to:

The GFD Fellowship Committee
Education Office, Clark Laboratory, MS #31
Woods Hole Oceanographic Institution
360 Woods Hole Road
Woods Hole, MA 02543-1541

Telephone: (508) 289-2950
Fax: (508) 457-2188
E-mail: gfd@whoi.edu
Internet: http://www.whoi.edu/education/gfd.html

Prospective senior visitors, please e-mail Jack Whitehead at: ***jwhitehead@whoi.edu***

The GFD Program is funded by the National Science Foundation and the Office of Naval Research

Molecular transport:

- Linear flux laws
- Coefficients are material parameters determined by microscopic interactions and thermodynamic state

Example

1. Heat transport

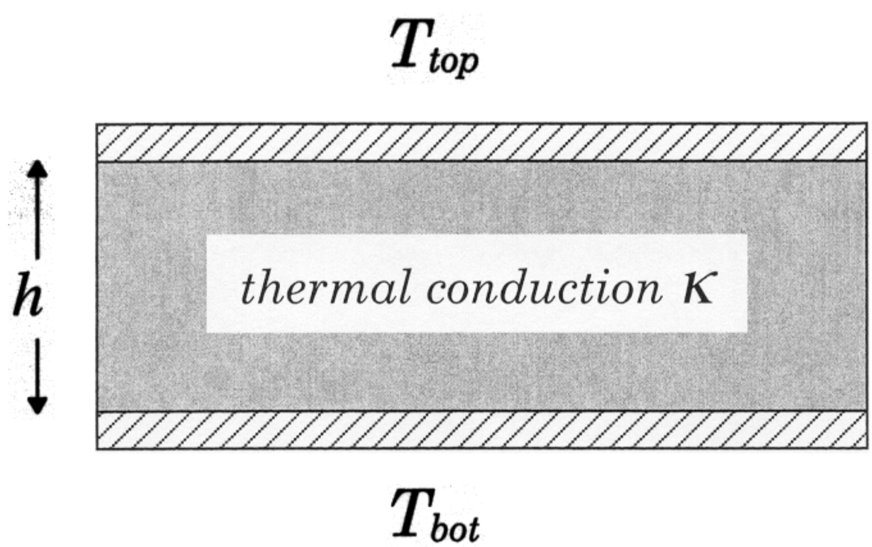

Vertical heat current: $J = \kappa\left(\frac{T_{bot} - T_{top}}{h}\right)$

Example

2. Momentum transport

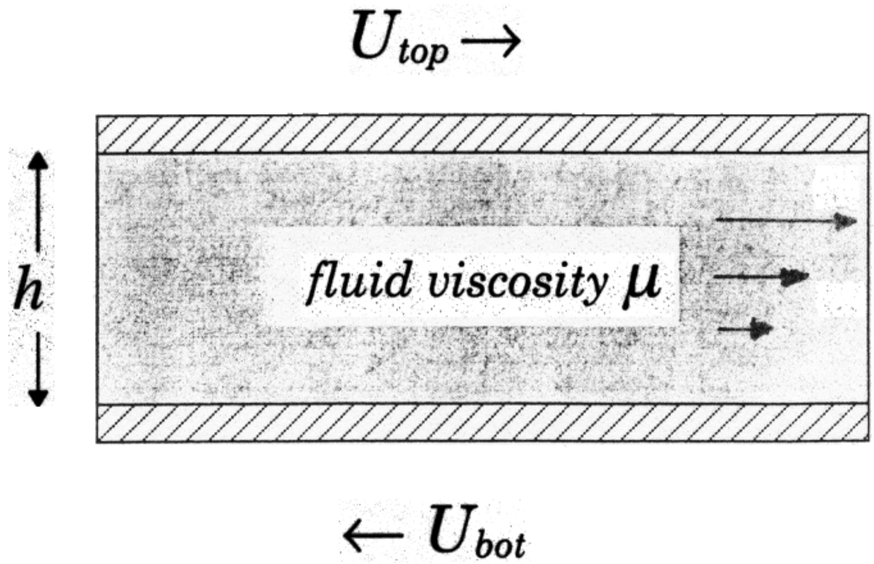

Vertical momentum current:

$$\tau = \frac{F}{A} = \mu \, \frac{U_{bot} - U_{top}}{h}$$

TURBULENT TRANSPORT:

- Enhanced transport due to fluid motion.
- Determined (in principle—we hope!) by macroscopic equations of motion.
- May hope for universal features in turbulent flows.

MATHEMATICAL QUESTIONS:

- What can be deduced *rigorously* from analysis of the equations of motion?
- How do such results compare with theoretical expectations and/or experimental observations?

ANSWERS: TBA

NOT DISCUSSED HERE:

- History of analysis and interesting technical issues ...

Momentum transport:

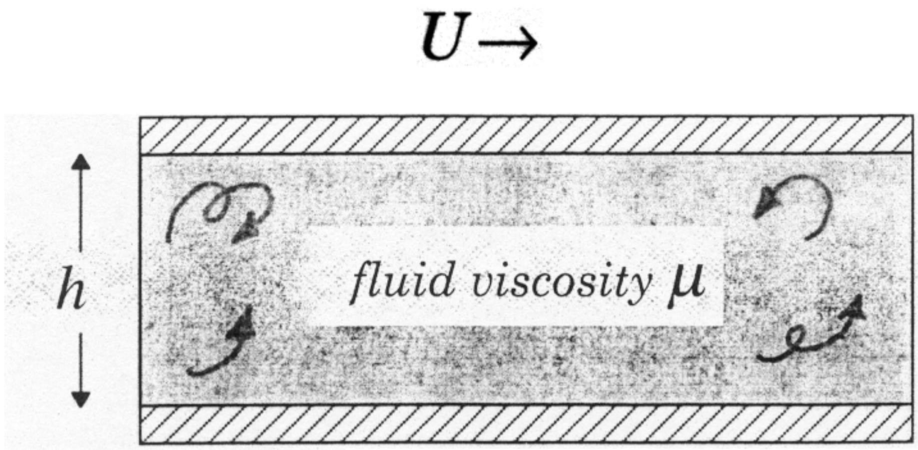

bottom at rest

- *Navier-Stokes equations* for $\mathbf{u}(x,\boldsymbol{t})$, $p(\mathbf{x},t)$:

$$\frac{\partial \mathbf{u}}{\partial t} + \mathbf{u}\cdot\nabla\mathbf{u} + \nabla p \quad \nu\Delta\mathbf{u}$$

$$\nabla\cdot\mathbf{u} = 0$$

+ no-slip boundary conditions

- *Kinematic viscosity*: $\nu = \dfrac{\mu}{\rho}$

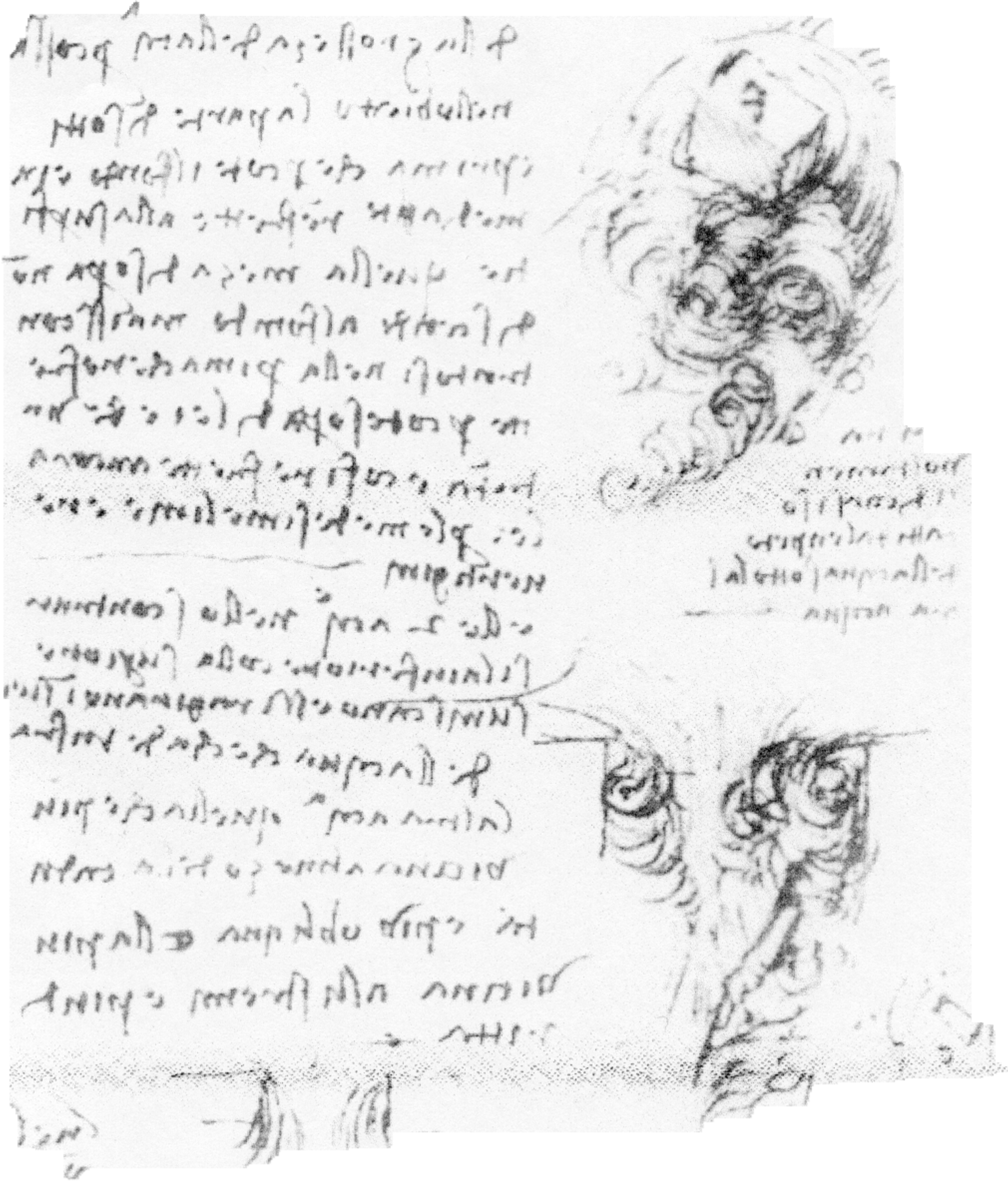

TURBULENCE

Uriel Frisch

5

Two experimental laws of fully developed turbulence

Experimental data will now be presented to illustrate two basic empirical laws of fully developed turbulence.

(i) **Two-thirds law.** *In a turbulent flow at very high Reynolds number, the mean square velocity increment* $\langle(\delta v(\ell))^2\rangle$ *between two points separated by a distance* ℓ *behaves approximately as the two-thirds power of the distance.*[1]

(ii) **Law of finite energy dissipation.** *If, in an experiment on turbulent flow, all the control parameters are kept the same, except for the viscosity, which is lowered as much as possible, the energy dissipation per unit mass* dE/dt *behaves in a way consistent with a finite positive limit.*

These laws seem to hold, at least approximately, for almost any turbulent flow. Let us now examine examples of such data.

"Kolmogorov" scaling

Vision of the "Turbulent Cascade":

high ν, low Uh/ν

$$\epsilon \sim \nu \frac{U}{h} \cdot \frac{U}{h} = \nu \frac{U^2}{h^2}$$

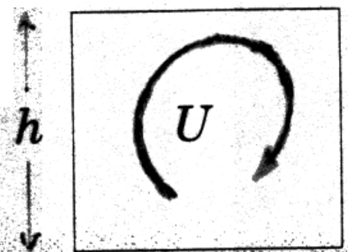

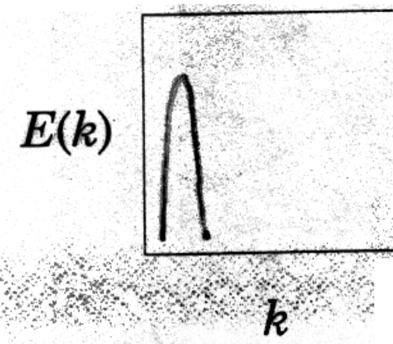

↓ ν, ↑ Uh/ν

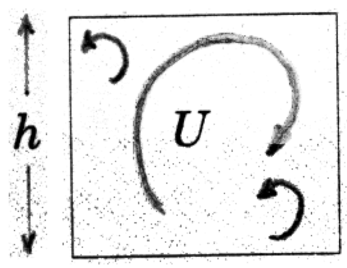

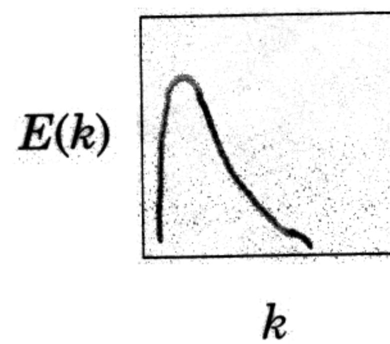

low ν, high Uh/ν

$\epsilon \sim ?$

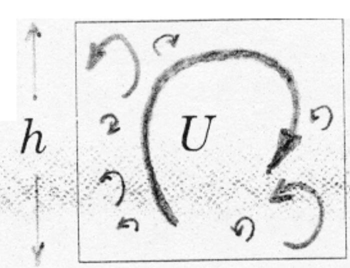

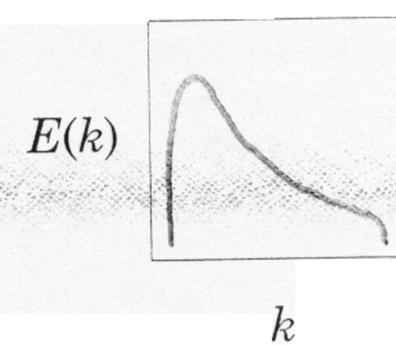

Energy input at large scales ⇒ "Cascades" to small scales

IN THE LIMIT OF *VERY* LOW VISCOSITY:

(OR VERY *HIGH* Uh/ν)

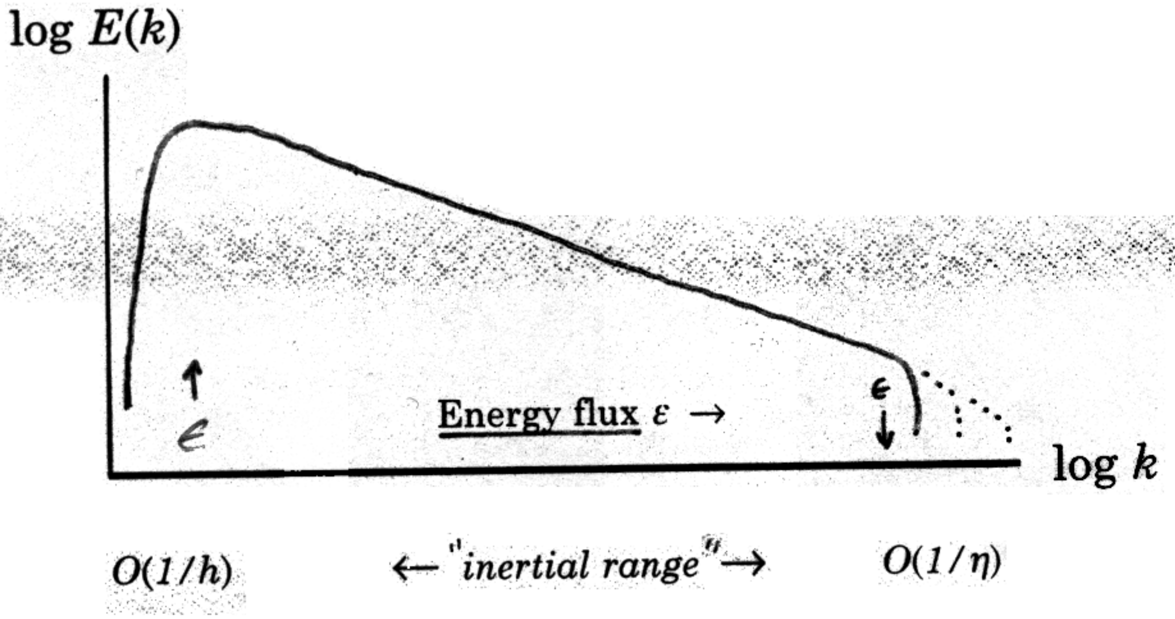

If inertial range spectrum does *not* depend on ν, then

$$E(k) \quad \varepsilon^{2/3} k^{-5/3}$$

Kolmogorov dissipation (small) scale: $\eta \sim (\nu^3/\varepsilon)^{1/4}$

$$\text{Total kinetic energy} \sim U^2 \quad \int_{O(1/h)}^{O(1/\eta)} E(k)\, dk \sim \varepsilon^{2/3} h^{2/3}$$

$\Rightarrow$ *"residual dissipation"* $\varepsilon \sim U^3/h$

ENERGY DISSIPATION RATE PER UNIT MASS:

$$\varepsilon = \frac{\nu}{hA} \left\langle \int |\nabla \mathbf{u}|^2 \, d^3x \right\rangle \leftarrow \text{space-time average}$$

POWER BALANCE:

$$\rho \times \varepsilon = \tau \times \frac{U}{h}$$

REYNOLDS NUMBER:

$$R = \frac{Uh}{\nu}$$

TRANSPORT ENHANCEMENT FACTOR:

$$N = \frac{\tau}{\rho \nu U/h} \qquad \frac{\varepsilon}{\nu U^2/h^2}$$

"KOLMOGOROV" SCALING

ε, τ *become independent of* ν *as* $R \to \infty$

$$\varepsilon \sim \frac{U^3}{h} \Leftrightarrow \tau \sim \rho U^3 \Leftrightarrow \boxed{N \sim R}$$

THEOREM: (Howard 1963 with statistical hypotheses

P.C. & C.R.D. 1992 without)

$$N \leq cR$$

EXPERIMENTS:

$$N \sim \frac{R}{(\log R)^2}$$

(Prandtl-von Karman log friction law, circca 1935)

IDEA OF THE ANALYSIS:

"background" profile

$$\mathbf{u}(\mathbf{x},t) = \hat{\imath}B(y) + \mathbf{v}(\mathbf{x},t)$$

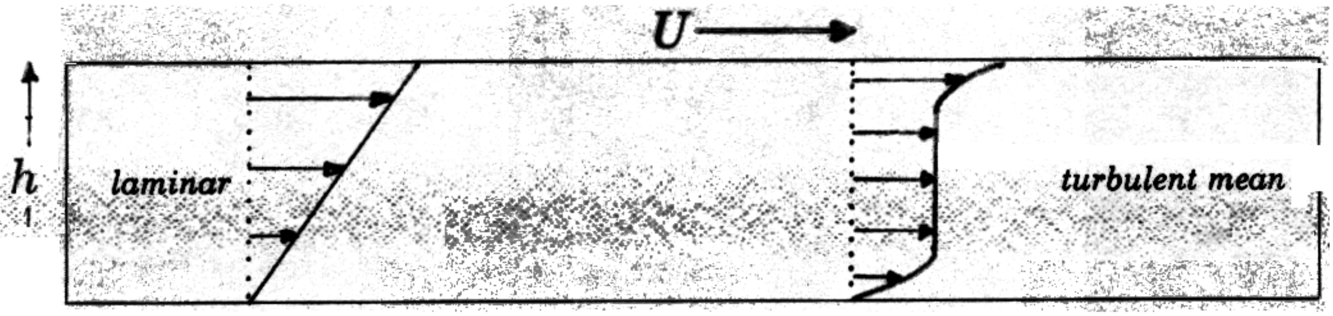

$$B(1) - B(0) = U \quad \& \quad \mathbf{v}(\mathbf{x},t) = 0 \text{ on boundaries}$$

(HOPF 1941)

B(y) not (necessarily) the mean profile

THEN:

$$\varepsilon = \frac{\nu}{hA}\left\langle \int |\nabla \mathbf{u}|^2 \, d^3x \right\rangle$$

$$= \frac{\nu}{h}\int_0^h B'(y)^2 dy - \frac{1}{hA}\left\langle \int \{\nu|\nabla \mathbf{v}|^2 + B'(y)v_1v_2\} \, d^3x \right\rangle$$

$$\leq \frac{\nu}{h}\int_0^h B'(y)^2 dy$$

IF the quadratic form is non-negative; that depends on $B(y)$.

Turbulent Flow between Concentric Rotating Cylinders at Large Reynolds Number

Daniel P. Lathrop, Jay Fineberg, and Harry L. Swinney
Center for Nonlinear Dynamics and Department of Physics, University of Texas, Austin, Texas 78712
(Received 13 September 1991)

Turbulent Taylor vortex flow is studied in experiments for Reynolds numbers $10^3 < R < 10^6$. Simple scaling of the torque with Reynolds number is *not* observed for any range of R, although the characteristic time scales and the transport of passive scalars are found to scale with the global torque measurements. Above a nonhysteretic transition observed at $R = 1.3 \times 10^4$, the torque has a Reynolds number dependence similar to the drag observed in wall-bounded shear flows such as pipe flow and flow over a flat plate.

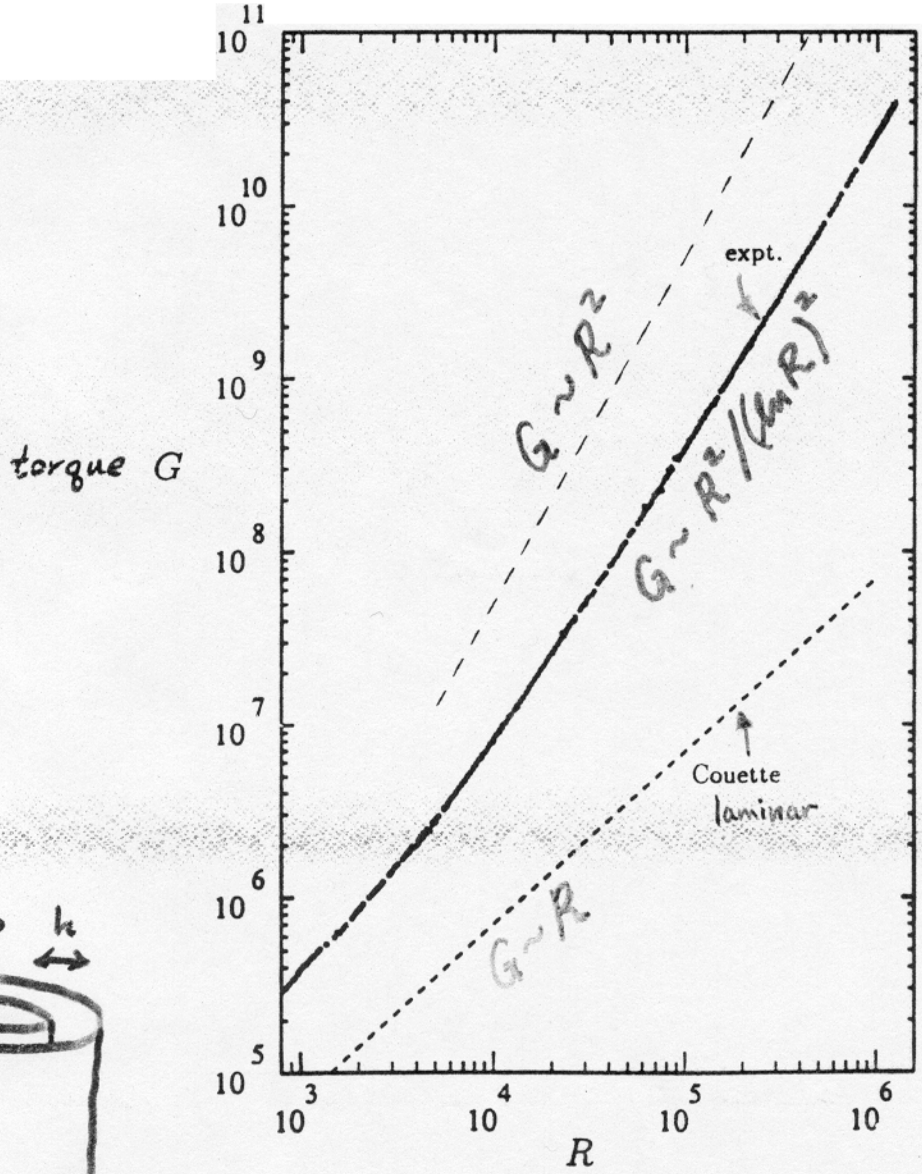

Best Prefactor for upper bound:

- Busse (1960s)
- Nicodemus et al (1990s)
- Kerswell et al (2002 preprint)

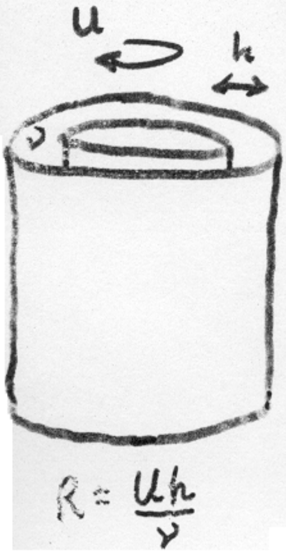

FIG. 11. A comparison of the measured nondimensional torque for eight vortices with the marginal stability prediction [Eq. (3)] [19,20], Couette flow torque [2], $G = 4\pi\eta[(1+\eta)(1-\eta)^2]^{-1}R$, and the Kolmogorov-type prediction [Eq. (5)].

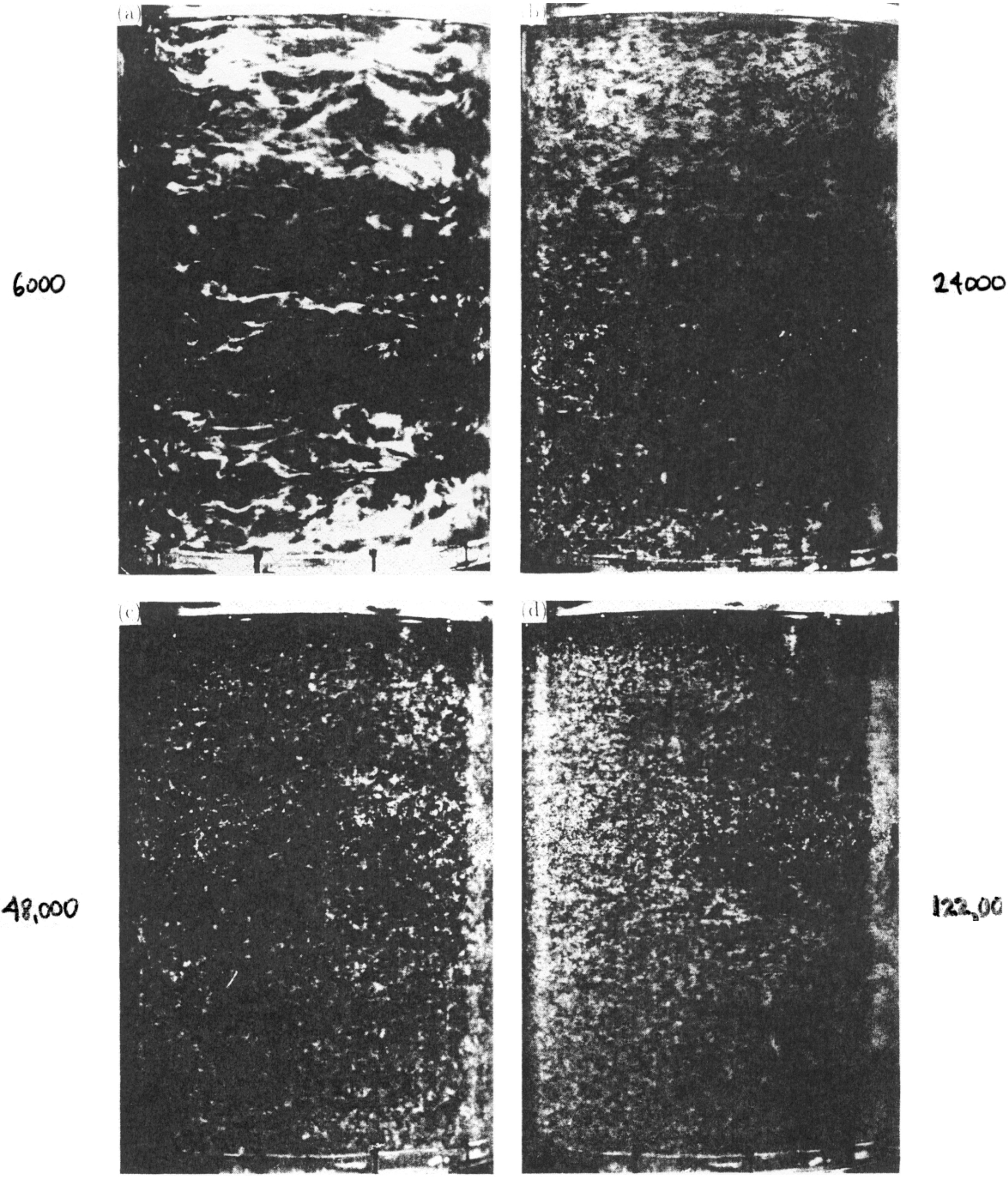

FIG. 5. Photographs of flow states at (a) $R = 6000$, (b) $R = 24\,000$, (c) $R = 48\,000$, and (d) $R = 122\,000$, obtained using Kalliroscope flow visualization. Eight vortices are visible in (a) and (b) and possibly (c), but not in (d).

VARIATION ON THE THEME: *Shear & suction*

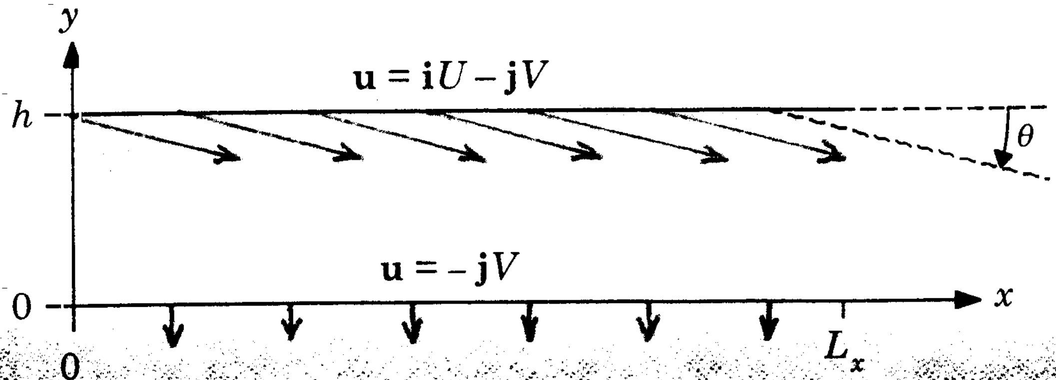

- **REYNOLDS NUMBER:**

$$R = \frac{Uh}{\nu}$$

- **INJECTION ANGLE:**

$$\tan\theta = \frac{V}{U}$$

- **EXACT STEADY SOLUTION:**

$$u_x(y) = U\,\frac{1 - e^{-Vy/\nu}}{1 - e^{-R\tan\theta}}$$

$$u_y = -V$$

$$u_z = 0.$$

Streamlines for the steady exact solution at Reynolds number $R = 100$ and various angles: (*a*) $\theta = 0$, planar Couette flow; (b) $\theta = .9^{\circ}$ with $\delta_{laminar} = .64h$; (c) $\theta = 9^{\circ}$ with $\delta_{laminar} = .064h$.

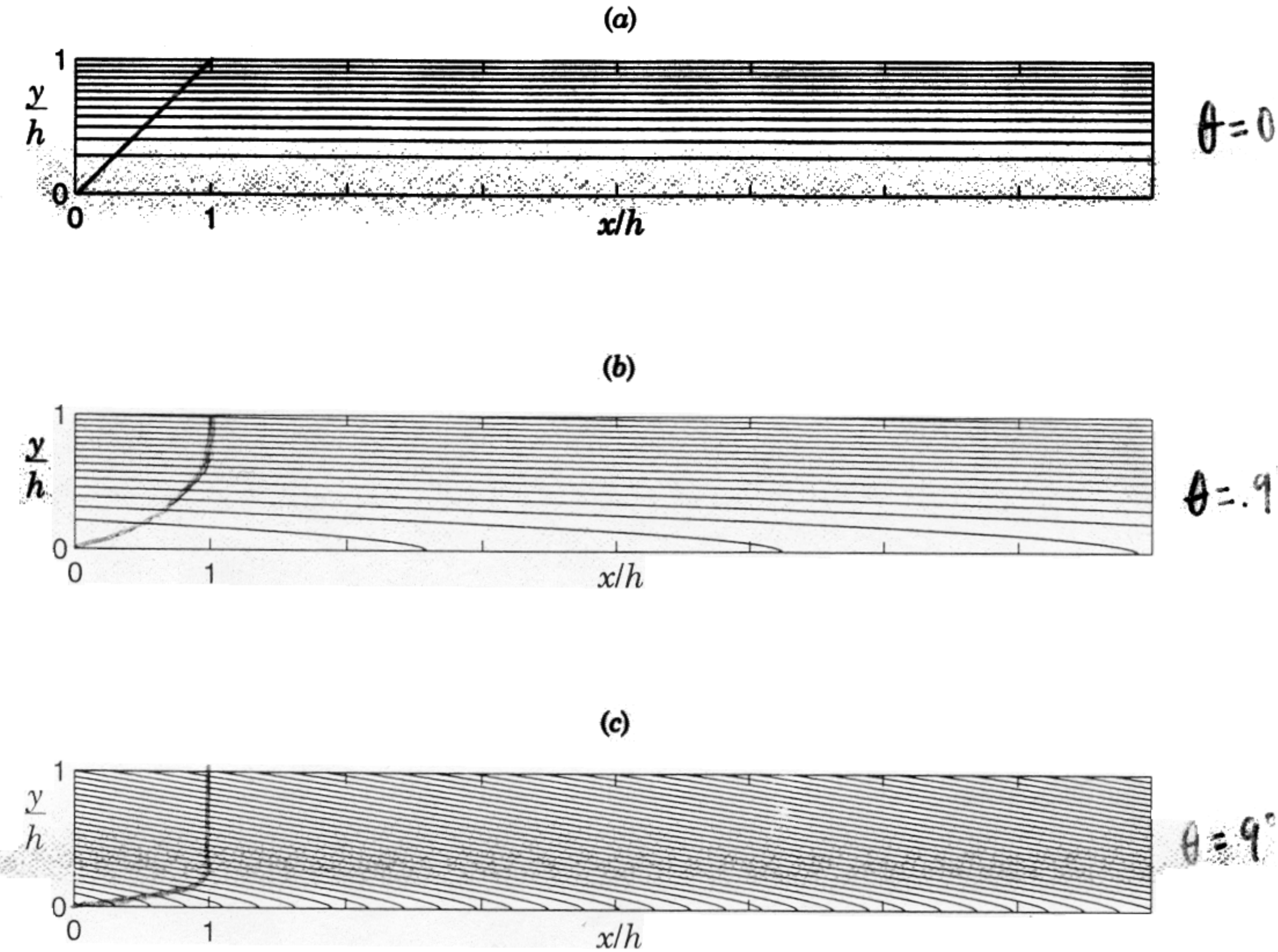

FACTS:

- **For steady laminar flow,**

$$\varepsilon_{laminar} \sim \frac{\tan\theta}{2}\frac{U^3}{h} \quad \text{as} \quad \nu \to 0 \quad (\text{for } \theta \neq 0)$$

- **Theorem** (C.D., Spiegel & Worthing 2000):

$$\varepsilon \leq \frac{1}{2\sqrt{2}}\left(1 + \frac{8}{3}\tan^2\theta\right)\frac{U^3}{h} \quad \text{as } \nu \to 0.$$

∴ $\nu \to 0$ scaling is sharp (for fixed $\theta \neq 0$)

Stability boundaries for the laminar flow:

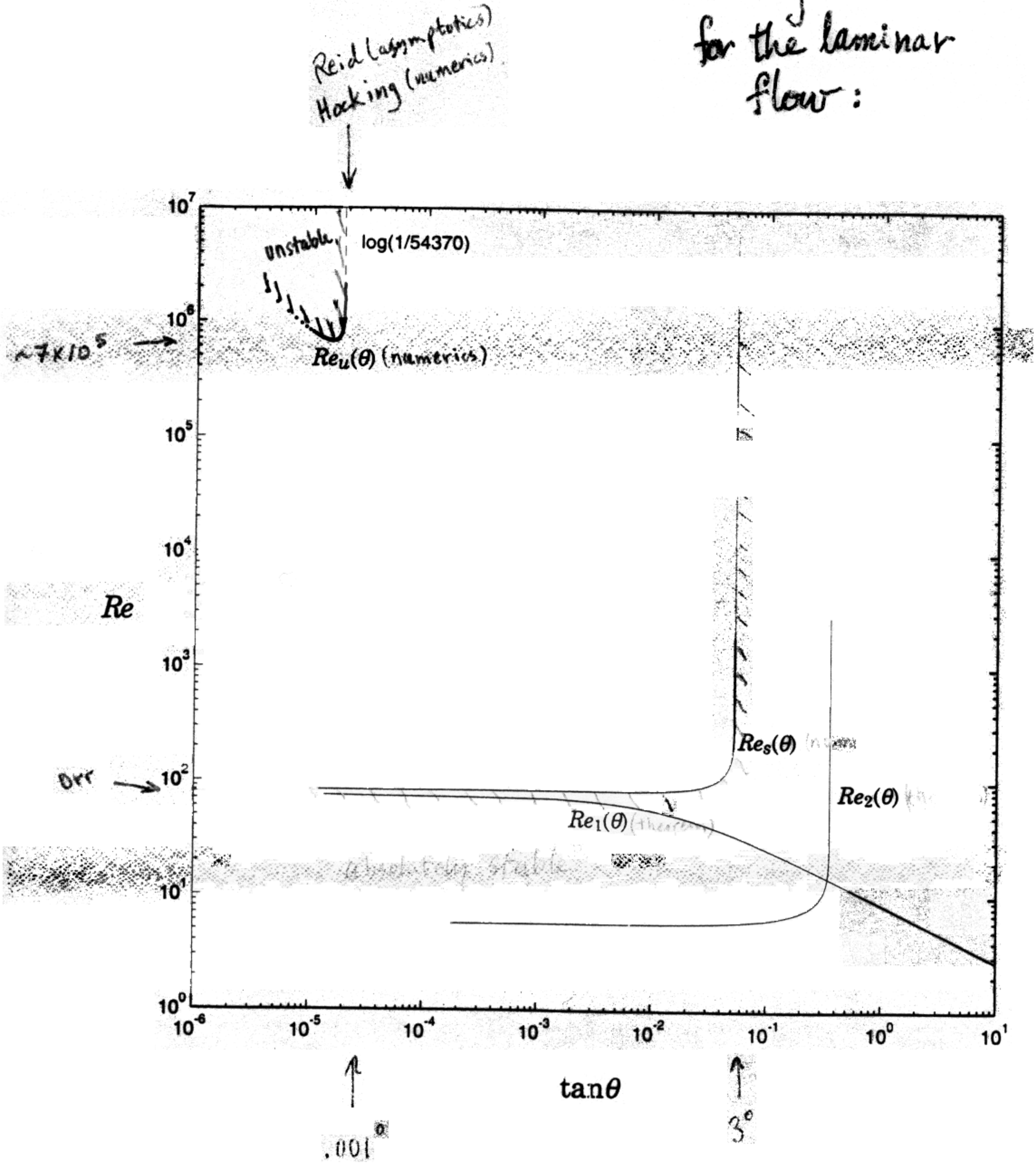

Results

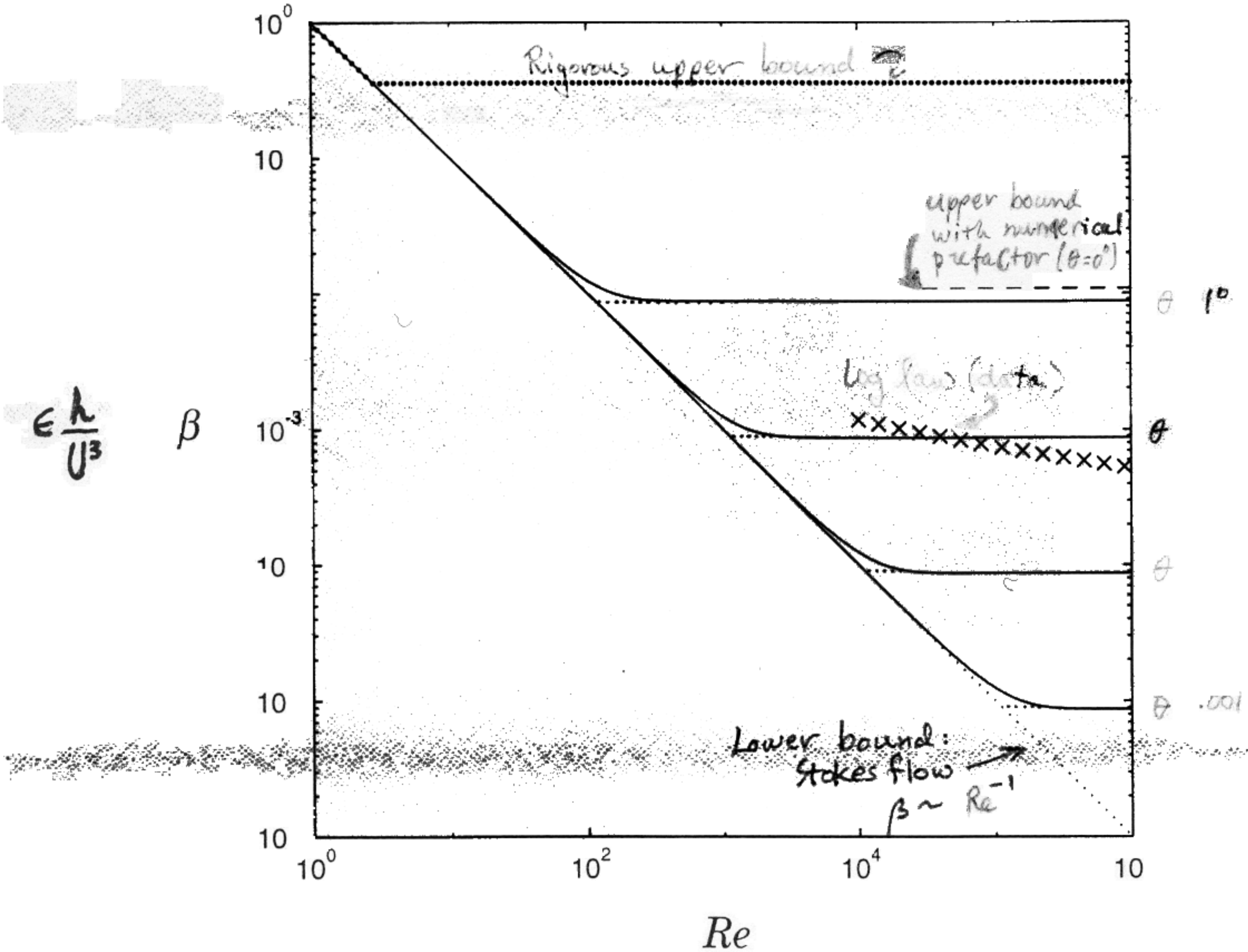

Conclusion upper bound analysis sha[illegible]
with respect to scaling

Question Can turbulent energy dissipation be less than laminar?

PHYSICAL REVIEW E VOLUME 56, NUMBER 1 JULY 1997

Energy injection in closed turbulent flows: Stirring through boundary layers versus inertial stirring

O. Cadot,* Y. Couder, A. Daerr, S. Douady, and A. Tsinober†
Laboratoire Physique Statistique, Ecole Normale Supérieure, 24 rue Lhomond, 75231 Paris, France
(Received 26 September 1996)

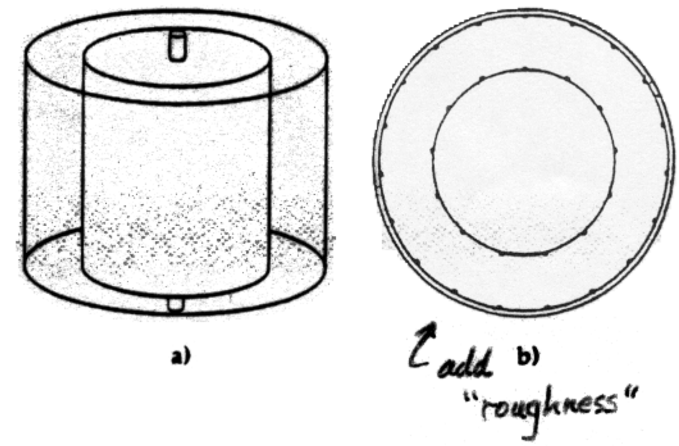

FIG. 4. Schemes of experiment B: (a) the Couette-Taylor cell with smooth surfaces and (b) the section of the system perpendicular to the axis of rotation and showing the ribs which make the walls rough.

In the following we will use a nondimensional rate of energy dissipation,

$$\beta_D = \varepsilon_D \frac{L}{U^3},$$

where U and L will be associated with the large scale motion of the turbulent flow.

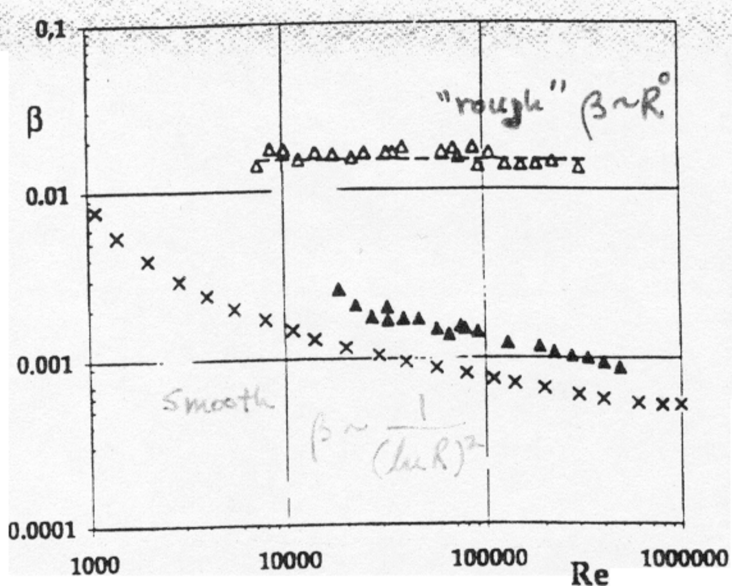

FIG. 5. Couette-Taylor experiments. Logarithmic plots of th nondimensional rates of energy dissipation β_D as a function of th Reynolds number. The black triangles (▲) are the results obtaine with smooth cylinders, and the open ones (△) correspond to thos obtained with the ribbed ones. The crosses (×) show for compari son the rates of energy injection β_D deduced from the data obtaine with smooth cylinders by Lathrop, Finenberg, and Swinney [8].

experimental data on the friction factor. This was used by Stanton[6] (1914) and consists of a logarithmic plot of friction factor against Reynolds number, with surface roughness the parameter as in Fig. 9.9. From such a plot, complete data on the friction factor can be obtained for laminar and turbulent flow of any fluid in smooth or rough pipes.

The results of the previously cited systematic tests by Nikuradse[7] on turbulent flow in smooth and rough pipes demonstrate perfectly the relationship among f, **R**, and relative roughness. In these tests geometric similarity of the roughness pattern was obtained by fixing a coating of uniform sand grains to a smooth pipe wall; thus the diameter of the sand grain e became the easily measurable index for the roughness. Although the sand-grain roughness of Nikuradse is quite different from that of commercial pipes (see Fig. 9.7), the former is an easily measured, definite quantity which provides a reliable basis for quantitative measurement of roughness effects; Nikuradse's results are generally accepted today as the basic standard for this measurement. The test results when plotted logarithmically in Fig. 9.9 illustrate the following important fundamentals:[8]

1. The physical difference between the laminar and turbulent flow regimes is indicated by the change in the relationship of f to **R** near the critical Reynolds number of 2 100.

Pipe/Channel Flow:

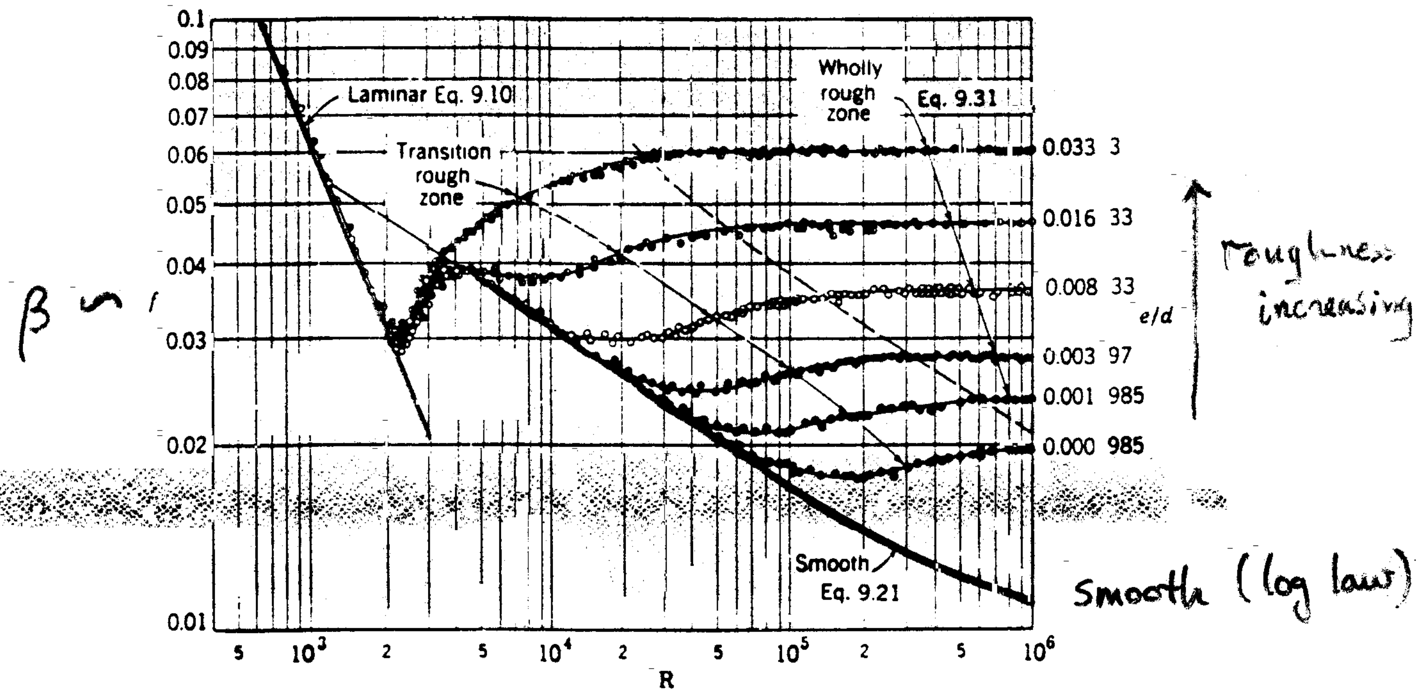

Fig. **9.9** Stanton diagram.

[6] It is generally known as a *Stanton diagram*.

[7] J. Nikuradse, "Strömungsgesetze in rauhen Rohren," *VDI-Forschungsheft*, 361, 1933. Translation available in N.A.C.A., *Tech. Mem.* 1291.

[8] Figure 9.9 is a summary of Nikuradse's test results. Curves drawn through the points have the equations indicated.

HEAT TRANSPORT:

$T = T_{top}$

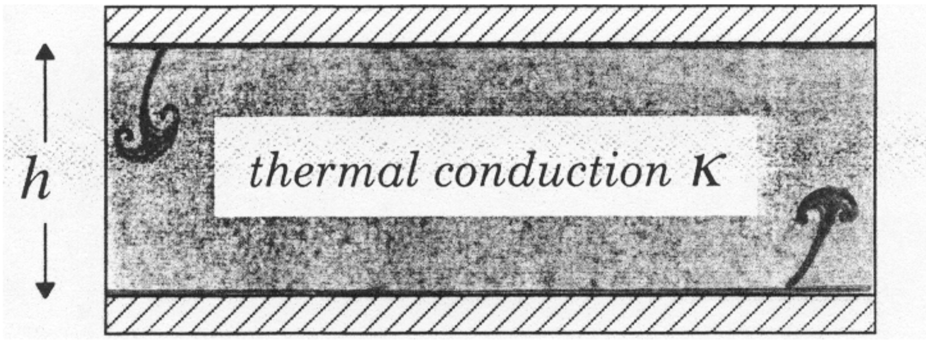

$T = T_{bot}$

- *Boussinesq equations* for $\mathbf{u}$, p, & $T(\mathbf{x},t)$:

$$\frac{\partial \mathbf{u}}{\partial t} + \mathbf{u}\cdot\nabla\mathbf{u} + \nabla p = \nu\Delta\mathbf{u} + \mathbf{k}g\alpha T$$

$$\nabla\cdot\mathbf{u} = 0$$

$$\frac{\partial T}{\partial t} + \mathbf{u}\cdot\nabla T = \kappa\Delta T$$

+ Temperature & no-slip boundary conditions

Rayleigh number:

$$Ra = \frac{g\alpha(T_{bot} - T_{top})h^3}{\nu\kappa}$$

Prandtl number:

$$Pr = \frac{\nu}{\kappa} \qquad (\textit{material parameter})$$

Vertical heat flux:

$$J = \mathbf{k} \cdot \frac{1}{hA} \left\langle \int (\mathbf{u}T - \kappa \nabla T) \, d^3x \right\rangle$$

Transport enhancement ⇔ Nusselt #:

$$Nu := \frac{J}{\kappa\,(T_{bot} - T_{top})/h} = \begin{matrix} \varepsilon h^4/\kappa^3 \\ Pr\ Ra \end{matrix}$$

"KOLMOGOROV" SCALING:

J becomes independent of ν, κ

$$\Updownarrow$$

$$Nu \sim (Pr\,Ra)^{1/2}$$

(Spiegel; Kraichnan 1962: $Pr^{-1/4}\,Ra^{1/2}$ with log corrections)

THEOREM:

$$Nu \leq c\,Ra^{1/2}$$

(Howard 1963 with statistical hypotheses

P.C. & C.R.D. 1996 without)

EXPERIMENTS:

$$Nu \sim \begin{cases} Ra^{1/3} \text{ for } t \leq \text{ mid 1980s} \\ Ra^{2/7} \text{ mid 80s} < t < \text{mid 90s} \\ Ra^{.309 - .5?} \text{ late 1990s} \leq t \leq \textit{present} \end{cases}$$

VARIATIONS ON THE THEME I:

- *2-d with free-slip boundary conditions*

$$\frac{\partial \mathbf{u}}{\partial t} + \mathbf{u}\cdot\nabla\mathbf{u} + \nabla p = \nu\Delta\mathbf{u} + \mathbf{j}g\alpha T$$

$$\nabla\cdot\mathbf{u} = 0$$

$$\omega = v_x - u_y \quad \Rightarrow \quad \omega_t + \mathbf{u}\cdot\nabla\omega = \nu\Delta\omega + g\,\alpha T_x$$

$$\frac{\partial T}{\partial t} + \mathbf{u}\cdot\nabla T = \kappa\Delta T$$

+ Temperature & no-stress/zero-vorticity boundary conditions

EXPECTATION:

$$Nu \sim Ra^{?}$$

CONJECTURE: (Otero & C.R.D. 2001)

$$Nu \leq c Ra^{.417 \approx 5/12}$$

VARIATIONS ON THE THEME II:

- *Infinite Prandtl number convection*

$$\boxed{Pr \to \infty \Rightarrow \mathbf{u} \text{ slaved to } T}$$

Stokes

$$\nabla p = \Delta \mathbf{u} + \mathbf{k} Ra T$$

$$\nabla \cdot \mathbf{u} = 0$$

$$\frac{\partial T}{\partial t} + \mathbf{u} \cdot \nabla T = \Delta T$$

+ Temperature & no-slip boundary conditions

EXPECTATION:

$$Nu \sim Ra^{1/3}$$

THEOREM: [P.C. & C.R.D. 1999 using L^∞ bound on $T(\mathbf{x},t)$]

$$Nu \le c Ra^{1/3} (1 + \log Ra)^{2/3}$$

VARIATIONS ON THE THEME III:

- *Porous medium convection*

Darcy's law & Temperature evolution

$$\mathbf{u} + \nabla p = \mathbf{k} Ra T$$ ← Darcy

$$\nabla \cdot \mathbf{u} = 0$$

$$\frac{\partial T}{\partial t} + \mathbf{u} \cdot \nabla T = \kappa \Delta T$$

+ Temperature & no-flow boundary conditions at walls

EXPECTATION FROM "KOLMOGOROV" SCALING:

J becomes independent of $\kappa \Leftrightarrow Nu \sim Ra$

THEOREM: (P.C. & C.R.D. 1998)

$$Nu \leq c Ra$$

J. Fluid Mech. (1990). *vol.* 214. *pp.* 287–320
Printed in Great Britain

An explanation for the multivalued heat transport found experimentally for convection in a porous medium

By C. R. B. LISTER
School of Oceanography, WB-10, University of Washington, Seattle, WA 98195, USA

(Received 18 April 1988 and in revised form 17 October 1989)

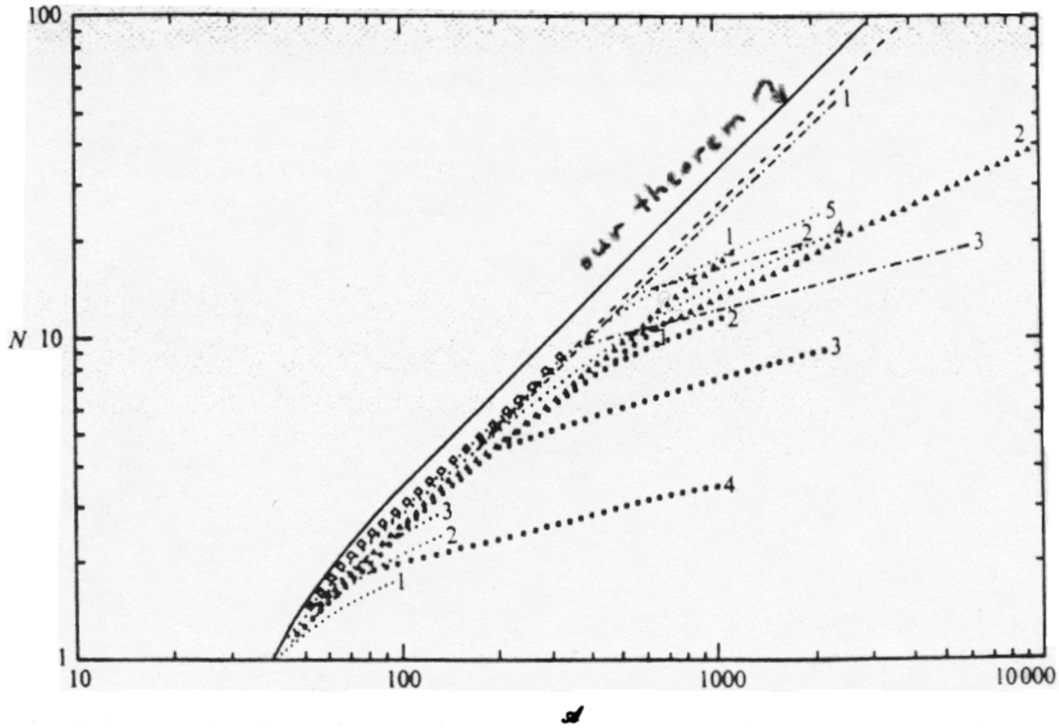

FIGURE 2. A representative compilation of published heat transport data, rescaled where necessary to show onset close to the theoretical critical Rayleigh number of $4\pi^2$ (Lapwood 1948). This value for the onset has been confirmed by a sensitive experiment in a Hele-Shaw cell (Hartline & Lister 1977); some published results differ owing to problems in measuring the physical properties of heterogeneous media. ——. A theoretical upper bound to the heat transport obtained with a variational method by Busse & Joseph (1972); their two-wavenumber solution takes off more steeply at a Rayleigh number of 280. ----, Hele-Shaw cell, thickness 4.75 mm, oil; 3, 5, 8 mm glass beads; 6 mm plastic balls; heights and configurations not given, except that the last, high-Rayleigh-number experiment was like an overgrown coffee percolator filled with foam plastic beads and water (Elder 1965). -·-·-, 1 = 'granular material'; 2 = 8 mm glass spheres; 3 = 18 mm glass spheres, no other data. A Hele-Shaw cell, height 2 cm, width 30 cm and thickness 6 mm, kerosene fill, followed curve 1 up to a Rayleigh number of 800 (Elder 1967). ·····, 1 = 1.9 mm quartz sand, water; 2 = 2.25 mm quartz sand, water and 4 mm lead balls, water; 3 = 1.9 mm quartz sand, oil; 4 = 1.7, 3.0, 4.0 mm glass beads, water; 5 = 0.9, 2.0 mm glass beads, oil and 4 mm polypropylene spheres, water; all depths 5.35 cm (Combarnous 1970). ◇◇◇, 3.25, 5.25 mm glass beads, water and 5.25 mm glass beads, silicone oil, no other data (Bories 1970). ■■■, 1 = 1 mm to 7 mm glass beads, water; 2 = 10 mm glass beads, water; 3 = 10 mm glass beads, turpentine; 4 = 15 mm steel balls, turpentine; height 4 cm (Schneider 1963). ▲▲▲, 1 = 3 mm glass beads, water, depth 4.3 cm and 6 mm glass beads, depth 8.6 cm; 2 = 14.3 mm glass beads, water, depth 8.8 cm (Buretta & Berman 1976). In these last three cases, the symbols are used only to make curves visibly separate: they are not data points.

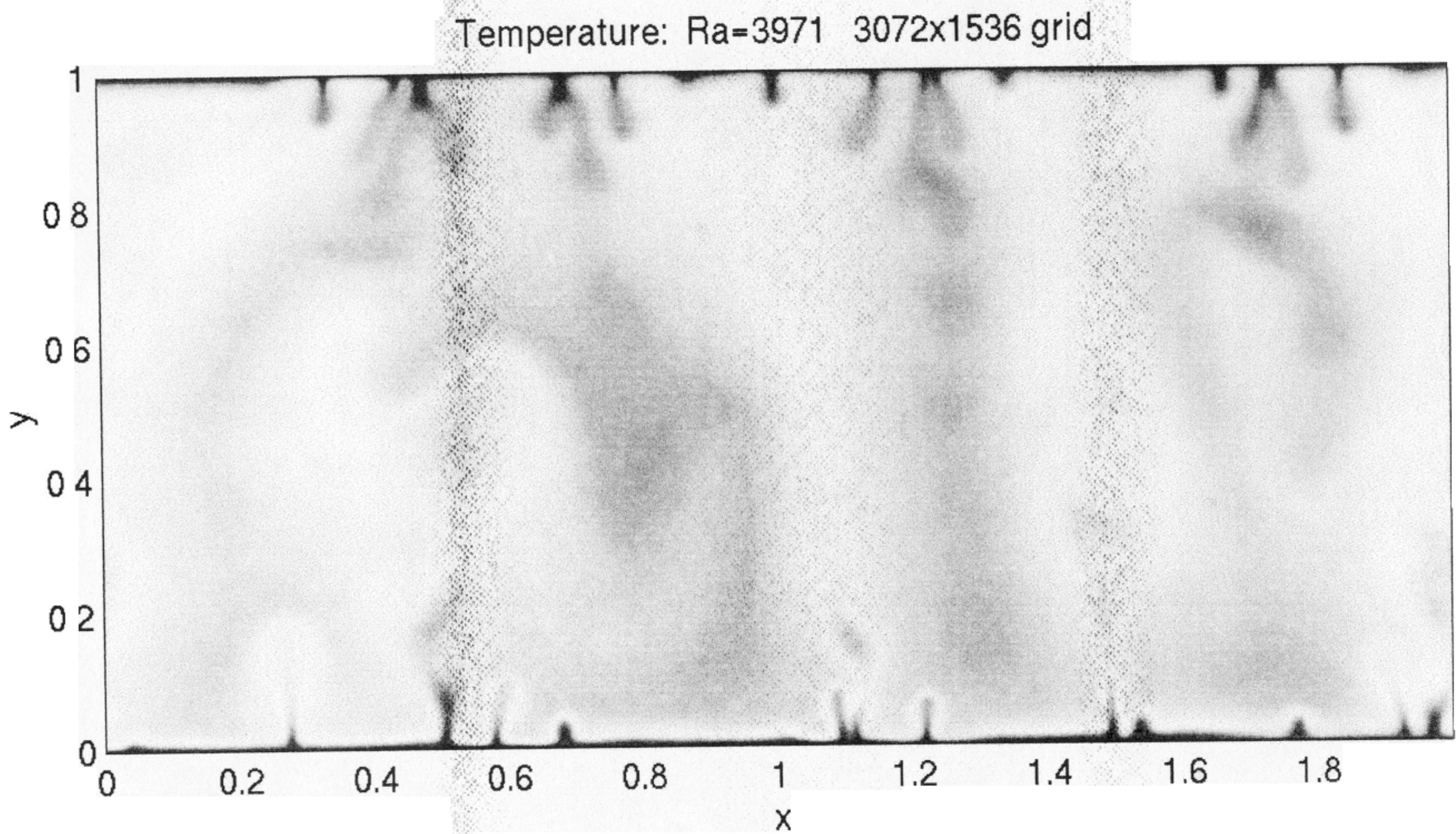

Temperature: Ra=3971 3072x1536 grid
y
0
0.2
0.4
0.6
0.8
1
0
0.2
0.4
0.6
0.8
1
1.2
1.4
1.6
1.8
x

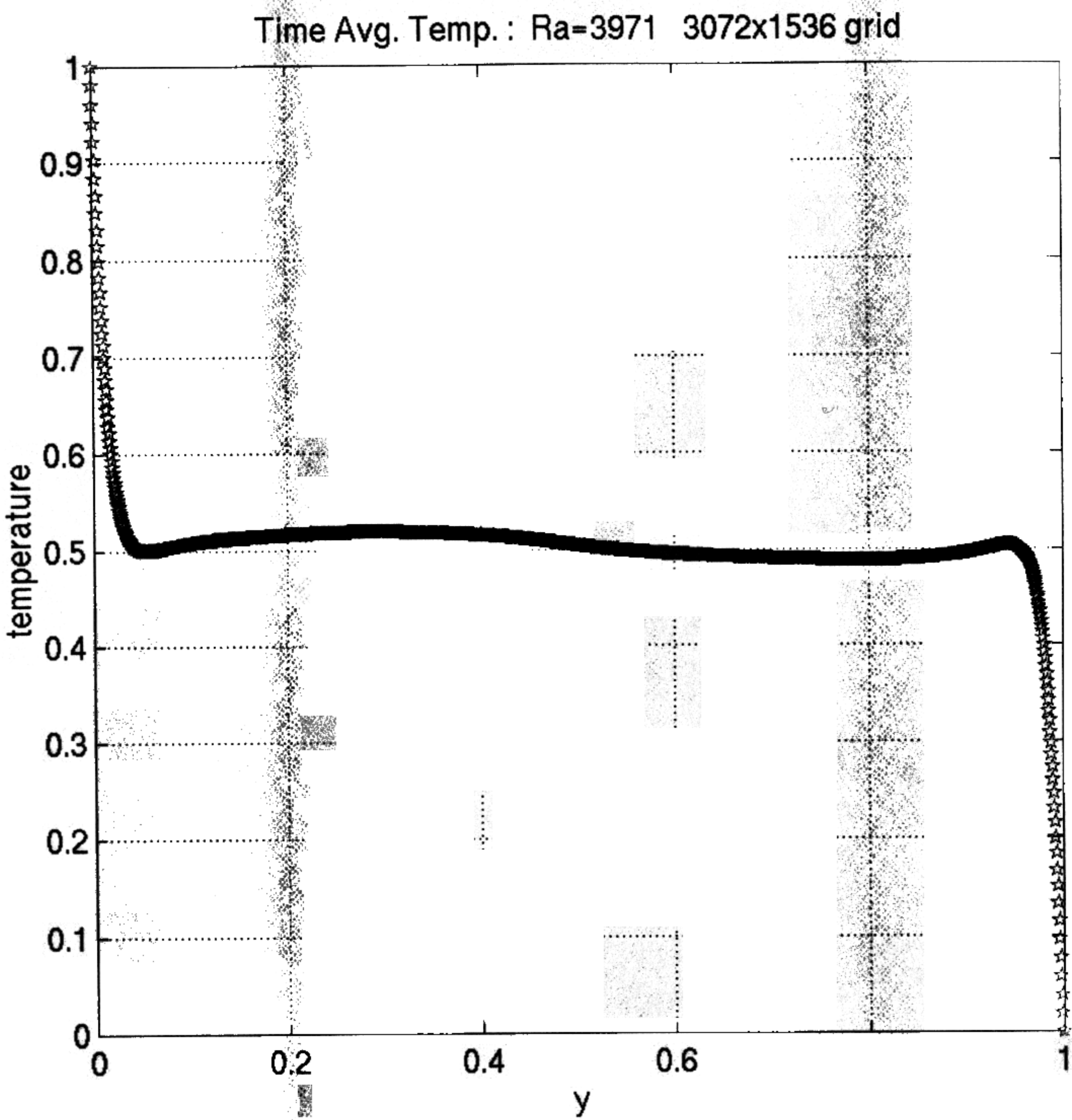
Time Avg. Temp. : Ra=3971 3072x1536 grid
temperature
y
0
0.1
0.2
0.3
0.4
0.5
0.6
0.7
0.8
0.9
1
0
0.2
0.4
0.6
1

Conclusions & Outlook:

In some cases . . . *Kolmogorov scaling*

- Finite transport in limit of vanishing material coefficients.
- Microscopic transport processes "renormalized" away.
- Turbulence tends to saturate rigorous mathematical limits (perhaps modulo logarithms).

However, *turbulent convection*

- is experimentally difficult.
- ... shows good agreement between analysis and observation only in some limiting cases.
- ... remains a challenge for mathematics, theory and experiments.

Other challenges:

- Other boundaries and boundary conditions.
- Effects of rotation.
- Open flows

FUNDAMENTALS OF PHYSICS

Third Edition

David Halliday
University of Pittsburgh

Robert Resnick
Rensselaer Polytechnic Institute

with the assistance of

John Merrill
Brigham Young University

WILEY

JOHN WILEY & SONS New York · Chichester · Brisbane · Toronto · Singapore

6-3 The Drag Force and Terminal Speed*

If a body moves through a fluid such as air or water, a frictionlike *drag force* will act on it, tending to retard its motion. We may be dealing with a cannon ball sinking in the ocean, a power boat crossing a lake, a truck driving along a highway, a bumblebee or a jet plane in flight, a baseball rising in the air, or a parachutist drifting down toward the earth. A typical small dust particle is so slowed down as it falls that it may take an hour to fall 1 ft. Since the air in our houses is never still, much dust never settles.

We limit ourselves to the case of bodies falling through air and moving at speeds high enough so that the flow of the air behind the falling body is turbulent. A falling baseball, sky diver, or parachutist meets these conditions. In these circumstances, the drag force acting on the body is given by

$$D = \tfrac{1}{2} C \rho A v^2. \qquad (16)$$

Here A is the effective cross-sectional area of the falling body, ρ is the density of air, and v is the speed of fall. C is a dimensionless *drag coefficient* that depends on the shape of the moving object and whose value generally lies in the range 0.5 – 1.0.

Power = Force x velocity $\sim \rho A v^3$

$\wr$

Energy dissipation rate ← does not depend on viscosity!

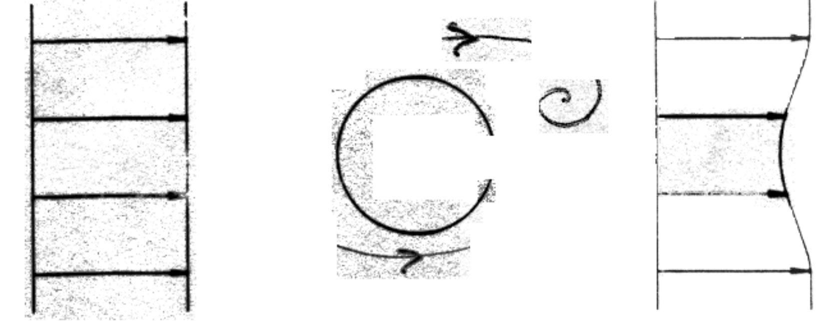

Fig. 3.14 Wake production: schematic velocity profiles upstream and downstream of an obstacle.

This anticipates ideas to be introduced in Chapter 7. It is plausible ahead of that discussion that, since the Reynolds number is being used to specify the conditions, results for D should be presented non-dimensionally; C_D is non-dimensional. This procedure does in fact enable all conditions to be covered by a single curve, shown in Fig. 3.15. The curve is based primarily on experimental measurements, too numerous to show individual points. At the low Re end the experiments can be matched to theory.

The corresponding plot between Reynolds number and drag coefficient can also be given for a sphere, although with less precision because of the experimental problem of supporting the sphere. The curve, although different in detail, shows all the same principal features as the one for the cylinder.

A few features of the curves merit comment, some of these being points to which we shall return in later chapters.

$\beta \sim$

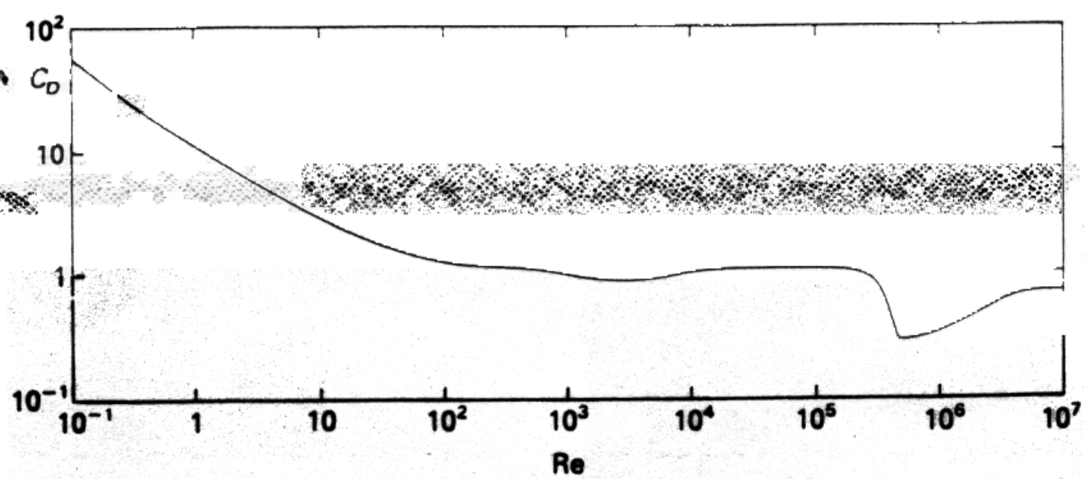

$\beta \sim Re$

Fig. 3.15 Variation of drag coefficient with Reynolds number for circular cylinder. Curve is experimental, based on data in Refs. [139, 159, 325, 370, 386, 410]. See also Refs. [204, 211].

Best rigourous estimate (2002): $\beta < O(e^{Re})$!

ou